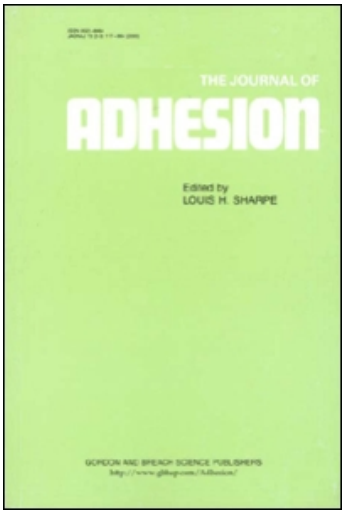

The Journal of Adhesion
Publication details, including instructions for authors and subscription information:
http://www.informaworld.com/smpp/title~content=t713453635

Local Stress Analysis of the Fatigue Behaviour of Adhesively Bonded Thick Composite Laminates

A. Bernasconi[a]; S. Beretta[a]; F. Moroni[b]; A. Pirondi[b]
[a] Politecnico di Milano, Dipartimento di Meccanica, Milano, Italy [b] Università degli Studi di Parma, Dipartimento di Ingegneria Industriale, Parma, Italy

Online publication date: 10 June 2010

To cite this Article Bernasconi, A. , Beretta, S. , Moroni, F. and Pirondi, A.(2010) 'Local Stress Analysis of the Fatigue Behaviour of Adhesively Bonded Thick Composite Laminates', The Journal of Adhesion, 86: 5, 480 — 500
To link to this Article: DOI: 10.1080/00218464.2010.484300
URL: http://dx.doi.org/10.1080/00218464.2010.484300

The Journal of Adhesion, 86:480–500, 2010

ISSN: 0021-8464 print/1545-5823 online
DOI: 10.1080/00218464.2010.484300

Taylor & Francis
Taylor & Francis Group

Local Stress Analysis of the Fatigue Behaviour of Adhesively Bonded Thick Composite Laminates

A. Bernasconi[1], S. Beretta[1], F. Moroni[2], and A. Pirondi[2]
[1]Politecnico di Milano, Dipartimento di Meccanica, Milano, Italy
[2]Università degli Studi di Parma, Dipartimento di Ingegneria Industriale, Parma, Italy

Results of fatigue tests on adhesive lap joints of thick (9.9 mm) composite laminates are presented and discussed. Specimens of different overlap length (from 25 to 110 mm), different shape, (with and without taper), and different materials (composite on composite, composite on steel) were fatigue tested and distinct fatigue curves were obtained in terms of maximum applied force and number of cycles to failure. In order to investigate the relationship between peak elastic stresses in the adhesive layer and fatigue life, a 2-D structural analysis of the joints by the finite element method was performed. The analysis evidenced a close relationship between the peak elastic stresses and the number of cycles to failure in the all-composite joints, as all experimental points in terms of peak shear (or Tresca) stress and number of cycles to failure collapsed within a band of relatively low scatter, irrespective of the shape of the joint and the overlap length. This behaviour suggested that peak elastic stresses in the adhesive layer could be adopted as a design criterion, at least as an engineering tool for industrial applications. In order for this method to be applied to the design of real components made of thick composite laminates, the sensitivity of the model results to the number and type of elements used to model the adhesive layer (solid or cohesive) was investigated and results compared. The limitations of the proposed approach with reference to the role of crack propagation are also discussed.

Keywords: Adhesive joints; Composite materials; Fatigue; Finite element method; Local stresses

Received 22 June 2009; in final form 15 March 2010.
Presented in part at the 3rd International Conference on Advanced Computational Engineering and Experimenting (ACE-X 2009), Rome, Italy, 22–23 June 2009.
Address correspondence to A. Bernasconi, Politecnico di Milano, Dipartimento di Meccanica, Via La Masa 34, I-20156 Milano, Italy. E-mail: andrea.bernasconi@polimi.it

1. INTRODUCTION

Fatigue strength of adhesively bonded joints in composite materials is of great importance for numerous applications, where the high performance of mechanically efficient materials like composites is fully exploited by means of suitable joining techniques. In the case of the present research, adhesive lap joints were employed with the aim of achieving modularity in the construction of large composite structures made of thick carbon fibre laminates for beam-like components to be employed in the industry of civil construction equipment. Modularity allows for cost effective solutions, *e.g.*, smaller moulds can be built and exchanged across products platforms. Moreover, by joining smaller parts together, smaller autoclaves are required for curing of the composite parts. However, these advantages are counterbalanced by the necessity of investigating the fatigue behaviour of the joining solutions required, particularly for load bearing applications.

It is well known that fatigue design of adhesive composite joints cannot simply rely on load-life curves of standard test specimens, because it has been demonstrated [1] that the load bearing capacity of an adhesive joint cannot be expressed in terms of average stresses, *i.e.*, applied load divided by the surface area of the adhesive joint [2,3]. This proved to be true also in the case of fatigue loads normalized by dividing by the respective static strength values [4]. In the case of lap joints, stress concentrations are localized at the overlap ends, as well as stress singularities at the interface between the adherends and the adhesive layer, whose intensity is not related to the average stress by a proportional law. Thus, transferring of the fatigue test results to the actual application requires a detailed analysis of the local conditions.

The approaches published so far can be divided into three main groups: criteria based on the local stress distributions [5], fracture mechanics based methods—which represent the most widely applied concept [6–8], and approaches adopting the generalized stress intensity factor (SIF) concept [9,10]. Fracture mechanics and SIF methods often display a good correlation with experimental results. Moreover, by applying fracture mechanics concepts it is possible to take into account the fatigue damage phenomena typical of composite adhesive joints, like crack propagation inside the laminate, either by propagation within the first ply or by failure of the interface between the first and the second plies, or by a combination of these two crack propagation manners, with several crack path variations. By local stress methods, although some connections between the local stress approach and the fracture mechanics based approaches can be

established [11], only stresses within the adhesive layer are considered. Thus, these methods simply define a limit condition for the forces to be applied to the joints and cannot provide a detailed description of the actual phenomena taking place during testing and/or operation. However, approaches based on local stresses can be applied more easily as engineering tools, and as such the analysis proposed in this work has to be evaluated.

In this paper, results of fatigue tests conducted on adhesively bonded joints between composite laminates and also between steel and composite are analyzed in order to verify the possibility of defining a fatigue strength criterion based on a function of the local stress values, acting in the adhesive layer. Single lap shear joints of different shape and overlap length were fatigue tested and results were analyzed in terms of local stress components evaluated by the finite element method. A similar approach—based on analytical formulations of the local stresses—proved to be valid for the case of static strength of steel adhesive joints [12]. In the case of composite laminates, analytical formulae cannot be easily derived. Therefore, the finite element method was adopted to evaluate local stress components. Possible meshing solutions were experimented and discussed in light of their computational efficiency for the fatigue strength assessment of adhesive joints in actual structures.

2. EXPERIMENTAL

In order to test bonded lap joints displaying different values of the maximum stress components acting within the adhesive layer, four different joints were designed and manufactured, with differences in:

- overlap length, from 25.4 to 110.8 mm;
- adherend materials (composite on composite and composite on steel);
- shape of the adherend (without and with tapering).

2.1. Single Lap Joints

Shape and dimensions of the specimens are reported in Fig. 1, with the following acronyms indicating:

- LS 25.4—single lap shear joint with 25.4-mm overlap length, both adherends made of composite;
- LS 50.8—single lap shear joint with 50.8-mm overlap length, both adherends made of composite;

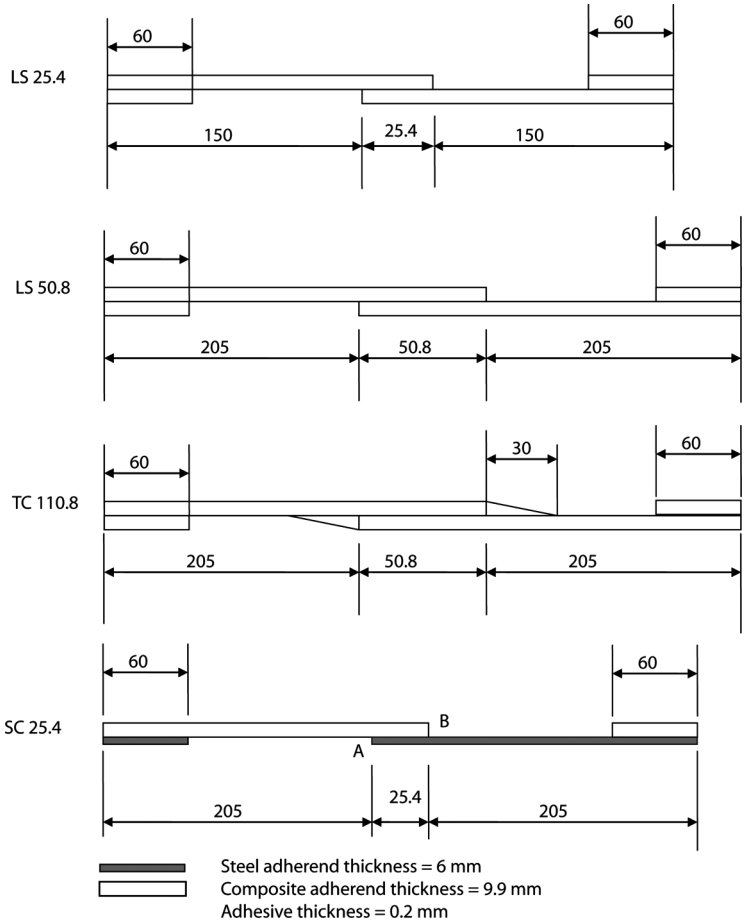

FIGURE 1 Shape and dimensions of the specimens (not to scale): width of all specimens is 25.4 mm.

- SC 25.4—single lap shear joint with 25.4-mm overlap length, one adherend made of composite, the other made of high-strength, low-alloy S690 steel;
- TC 110.8—single lap shear joint with 110.8-mm overlap length, both adherends made of composite, tapering of the adherends.

All specimens were 25.4 mm wide. Tapering of the adherends in TC 110.8 specimens was carefully manufactured in order to achieve an initial rise of 1 mm, as shown in Fig. 2. Although better

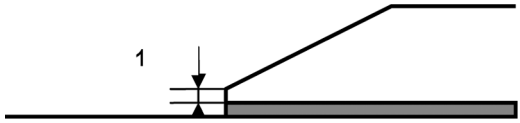

FIGURE 2 Details of the initial rise in tapered joints.

configurations exist, such as inside tapering with fillet, which allow for further reducing peel stresses [13], this detail closely reproduces the end of the overlap in the real part. All composite adherends were 9.9-mm thick laminates, having the same stacking sequence of woven and unidirectional low modulus carbon fibre and epoxy matrix pre-pregs. The stacking sequence is reported in Table 1. Joints were manufactured using a high-strength, two-component, ambient temperature curing, toughened epoxy adhesive (9323 B/A Structural Adhesive, 3M Italy). With the exception of LS 25.4 specimens, a uniform bond line thickness of 0.2 mm was achieved by means of calibrated copper wires inserted in the adhesive layer with a longitudinal orientation. The longitudinal orientation of wires is believed to minimize the stress concentration, although it is not completely stress free as is the case of other solutions, like small calibrated glass beads. However, specimens were tested in this configuration because it was the same solution which was planned to be adopted in the real part. Aluminium end tabs of the same thickness as the composite adherends were bonded to the specimens in order for the tensile loads to be applied in the mid plane of the adhesive layer. In the case of SC 25.4 specimens, composite end tabs of 9.9-mm thickness were bonded on the steel adherend and steel end tabs of 6-mm thickness were bonded to the composite adherend. Thus, in this case the tensile load was not centered on the mid surface of the adhesive layer and, consequently, the shear and peel stress distributions within the adhesive are not symmetric with respect to the centre of the glue line, as is the case of joints with adherends of equal thickness. In the SC 25.4 configuration, with reference to the sketch reported in Fig. 1, the maximum shear stress is located at the beginning of the overlap (point A), whereas the peak of the peel stress is found at the end of the overlap (point B).

TABLE 1 Stacking Sequence of the Composite Laminate (T, woven 0.66 mm thick; UD, unidirectional 0.33 mm thick)

T 45°/ UD_5 / T 0° / T 45°_2 / T 0°_2 / T 45°_2 / T 0° / UD_5 / T 45°

2.2. Bulk Adhesive Properties

Elastic properties of the 3M 9323 adhesive were determined on two bulk specimens moulded to the shape of ASTM D638-08 type IV specimens. Tensile tests were conducted and the axial strain was measured with both an axial extensometer and an electric resistance strain gage bonded to the specimen's surface. A second strain gage was bonded with transversal orientation in order to measure the Poisson's ratio. The stress-strain response of the bulk adhesive was almost linear up to failure, which took place in a brittle manner. The elastic constants $E = 2300\,MPa$ and $\nu = 0.33$ were obtained from the stress-strain curves.

2.3. FATIGUE TESTS

Tension to tension fatigue tests (load ratio $R = F_{min}/F_{max} = 0$) were conducted using a Schenck Hydropuls servo hydraulic testing machine of 250 kN capacity (Carl Schenck AG, Darmstadt, Germany). Tests were conducted in load control mode and interrupted at complete separation of the adherends. Loads were applied with a sinusoidal wave at the frequency of 2 Hz. Tests were conducted in an air conditioned environment at temperatures in the 23–26°C range, without control of relative humidity. With the exception of a few specimens, as reported in the following section, no monitoring of the crack propagation was performed. An average number of two specimens were tested for each load level, with a minimum of five load levels, selected in order to cover the range of 10^3 to 10^6 cycles to failure.

3. RESULTS

Fatigue tests results are reported in the graph of Fig. 3 as S-N curves, where the log(maximum applied force) values are reported on the ordinates and the log(number of cycles to failure) values, $\log(N_f)$, are reported on the abscissae. Each data point set was interpolated linearly and the corresponding interpolating lines are also reported in Fig. 3. Force values are normalized by dividing by the fatigue strength at 100,000 cycles to failure of LS 25.4 specimens, as derived from the line interpolating experimental results. By this normalization, the relative differences in fatigue strength of joints having different overlap length and other different features are clearly apparent in Fig. 3. It is, thus, confirmed that the effect of increasing overlap length does not correspond to an increase of overall fatigue strength of the joints proportional to the overlap length, as can be seen by comparing

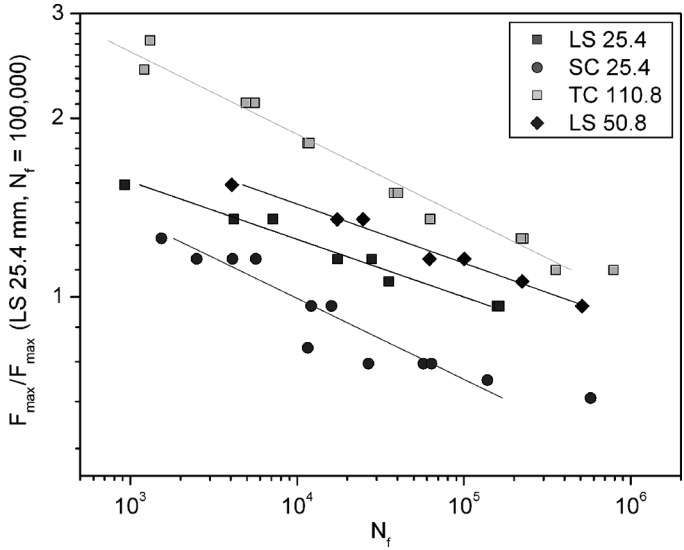

FIGURE 3 S-N curves reporting the relationship between number of cycles to failure and maximum applied forces; force values are normalized by dividing by fatigue strength of LS 25.4 joints at 100,000 cycles.

LS 25.4 and LS 50.8 S-N curves: an increase of the overlap length by a factor of 2 corresponds to an increase of the fatigue strength at 100,000 cycles by a factor of 1.2.

3.1. Fracture Surface Analysis

Inspection of fracture surfaces revealed that failure of LS 25.4 mm specimens was localized mainly in the adhesive layer, as shown in Fig. 4, with fewer evidences of crack propagation in the 45° ply, as shown in

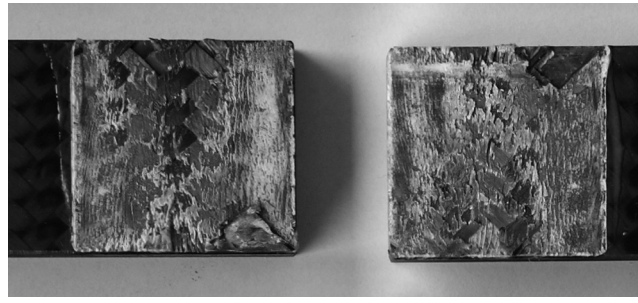

FIGURE 4 Fracture surface of a LS 25.4 joint.

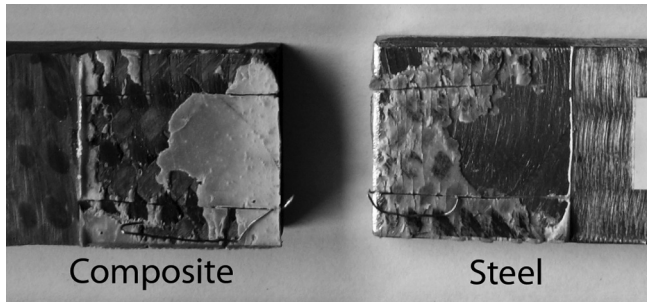

FIGURE 5 Fracture surface of a SC 25.4 joint.

the following paragraph. In the case of SC specimens, failure was localized at the interface between adhesive and steel, as shown in Fig. 5, and as confirmed by observations of the crack nucleation in two specimens of this type using an optical microscope. One of these pictures is reported in Fig. 6, where it clearly appears that the crack started at the end of the composite adherend overlapping the steel adherend (point B of Fig. 1). Longer joints, like LS 50.8 and TC 110.8, displayed a more complex behaviour. In the case of LS 50.8 joints, three out of ten specimens failed by interlaminar crack propagation between the 45° woven ply and the 0° unidirectional

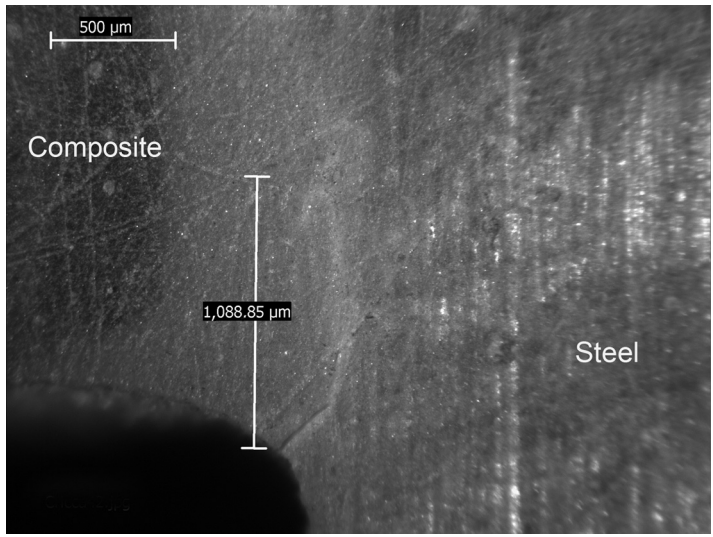

FIGURE 6 Optical microscope observation of the crack initiation site in a SC 25.4-joint ($F_{max} = 10$ kN, $N_f = 29{,}500$).

FIGURE 7 Fracture surfaces of LS 50.8 joints: (a) failure in the adhesive layer, (b) interlaminar failure.

ply (Fig. 7b), whereas the remaining specimens failed by crack propagation at the interface between composite and adhesive (Fig. 7a). Finally, all the specimens of the TC 110.8 series displayed a very complex crack path, always ending in an interlaminar crack propagation between the 45° woven ply and the 0° unidirectional ply, as described in the following paragraph.

3.2. Role of Crack Propagation

Crack propagation was not monitored during fatigue testing. In order to assess the role of crack propagation, some investigations were performed by monitoring the crack path using an optical microscope equipped with a CCD camera. Images of the crack front emerging on the side of specimens were acquired every 500 cycles (test was interrupted and the specimen was loaded up to the maximum force in the cycle in order to keep crack faces open). As shown in Fig. 8, in one LS 25.4 type specimen (test conditions $F_{max} = 13$ kN, $N_f = 17{,}200$), a small crack was already visible at an early stage (after 500 cycles) within the first ply, close to the edge of the upper adherend. This delamination propagated parallel to the ply surface for 12,500 cycles and at 16,000 cycles the crack path deviated into the adhesive layer, until final fracture. Final crack depth was approximately 7 mm before unstable crack propagation.

A different behaviour was observed in two TC 110.8 specimens. In the first one, (test conditions $F_{max} = 19$ kN, $N_f = 18{,}700$), as shown in Fig. 9, a crack nucleated within the adhesive layer starting from

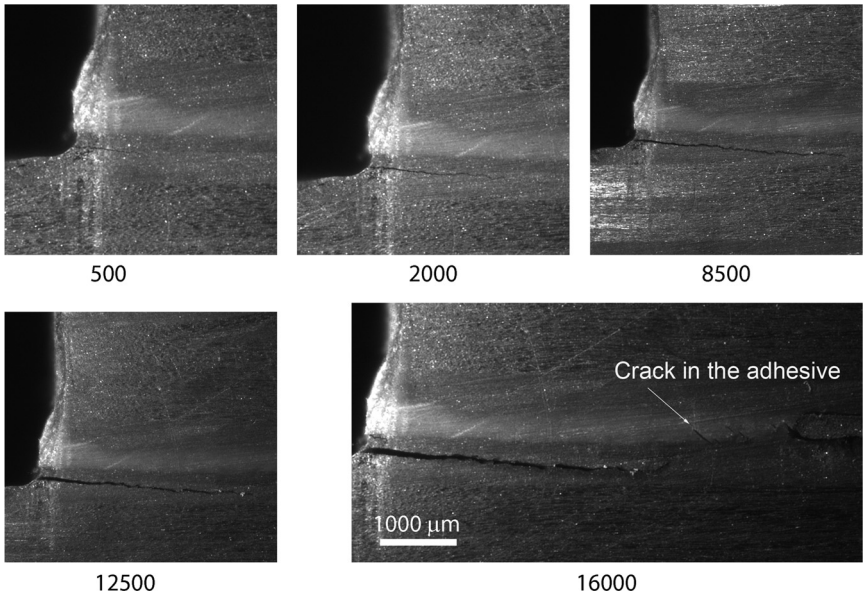

FIGURE 8 Crack propagation in a LS 25.4 joint ($F_{max} = 13$ kN, $N_f = 17{,}200$).

one end of the lap joint and propagated towards the interface between composite and adhesive during the first 9,000 cycles. Then the crack deviated into the first ply of the lower adherend and followed a

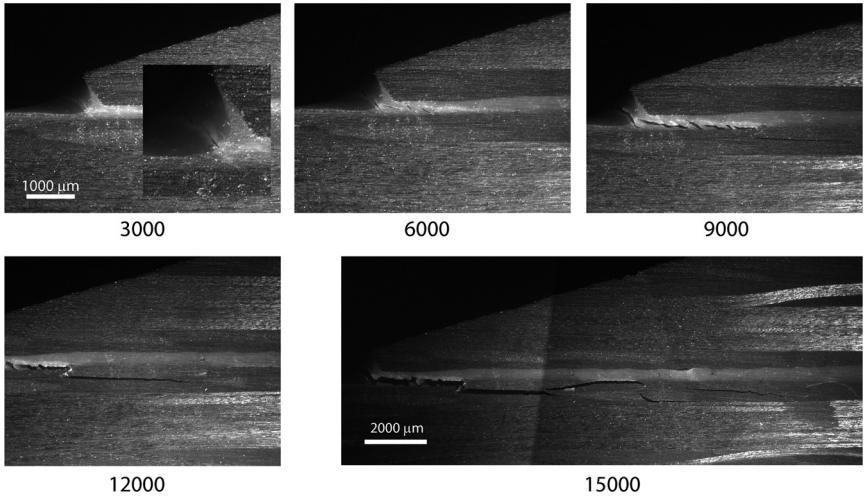

FIGURE 9 Crack propagation in a TC 110.8 joint ($F_{max} = 19$ kN, $N_f = 18{,}700$).

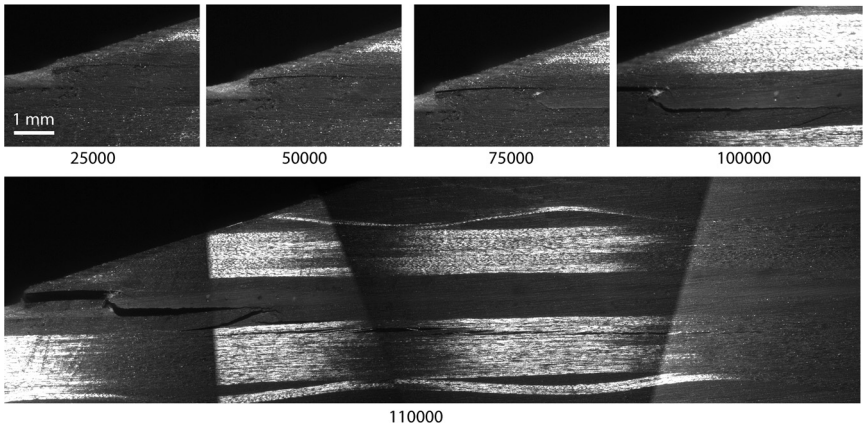

FIGURE 10 Crack propagation in a TC 110.8 joint ($F_{max} = 14$ kN, $N_f = 140{,}500$).

complex path, presumably following the texture of the woven material, until failure which took place with a final crack depth of 50 mm, before unstable crack propagation took place. A more complex behaviour was observed in the second TC 110.8 specimen (test conditions $F_{max} = 14$ kN, $N_f = 140{,}500$), as reported in Fig. 10: in this case the crack first nucleated in the first ply of the upper adherend after 3,000 cycles, and then followed a tortuous path consisting of failure of the interface between the adhesive and the lower adherend (up to 100,000 cycles), followed by propagation in the second ply (unidirectional) of the lower adherend until failure. Final crack depth was approximately 80 mm before unstable crack propagation.

These observations suggested that crack propagation had a dominant role in the fatigue behaviour of the joints we tested, particularly for longer joints, at least in the range of fatigue lives in the interval between 10,000 and 150,000 cycles. Fractions of the fatigue life required by crack initiation over total fatigue life, N_i/N_{TOT}, are reported in Table 2 (N_i corresponds to the number of cycles after which the first sign of a crack emerging on the side surface of the specimen

TABLE 2 Values of Fatigue Life Fraction N_i/N_{TOT} Required by Crack Nucleation

Joint type	N_{TOT}	Ni	N_i/N_{TOT}
LS 25.4	17200	500	0.03
TC 110.8	18700	3000	0.16
TC 110.8	140500	25000	0.18

was observed). Although observations did not cover all tests and we did not test thin joints made of the same composite and adhesive system, by comparing the values reported in Table 2 with the wider set of data reported in Ref [3]. concerning thinner (1.6 mm) joints of a similar adhesive-composite system, it could be inferred that fatigue crack initiation in thick composite joints might be shorter than that observed in thinner joints.

4. LOCAL STRESS ANALYSIS BY THE FINITE ELEMENT METHOD

The complexity of the fatigue behaviour of the tested joints was shown in the preceding sections and the dominant role of crack propagation was described. The analysis proposed in this section is based on the stress distribution calculated by finite element analysis in the adhesive layer only, irrespective of the actual nucleation site and crack path, and seeks a function of these stress components which allows for interpretation of fatigue test results. The purpose of this analysis is to provide a simple tool, useful for the preliminary fatigue assessment of adhesive joints for engineering applications. The approach neglects stress singularities and, considering peak elastic stresses within the adhesive only, it is not suitable for predicting the observed behaviour of fatigue cracks in this type of joint, particularly in the case of longer joint, displaying complex crack paths.

4.1. Finite Element Analysis

Joints were modelled using 2-D plane strain solid elements in Abaqus 6.7 (SIMULIA, Dassault Système, France). The composite layup was modelled by cutting the adherend section into several partitions corresponding to the different plies. An orthotropic material model with engineering constants of the corresponding ply was adopted for each partition. Values of the engineering constants are reported in Table 3. The adhesive was modelled using four quadratic elements in the thickness direction, having 0.05-mm edge length, with an homogeneous linear elastic constitutive model (values of the elastic

TABLE 3 Engineering Constants of the Unidirectional (UD) and Woven (T) Plies, with Reference to the Analysis' Coordinate System

Material	E_{11} (MPa)	E_{22} (MPa)	ν_{12}	G_{12} (MPa)
UD	104,000	8,000	0,24	3000
T	54,000	8,000	0,025	3000

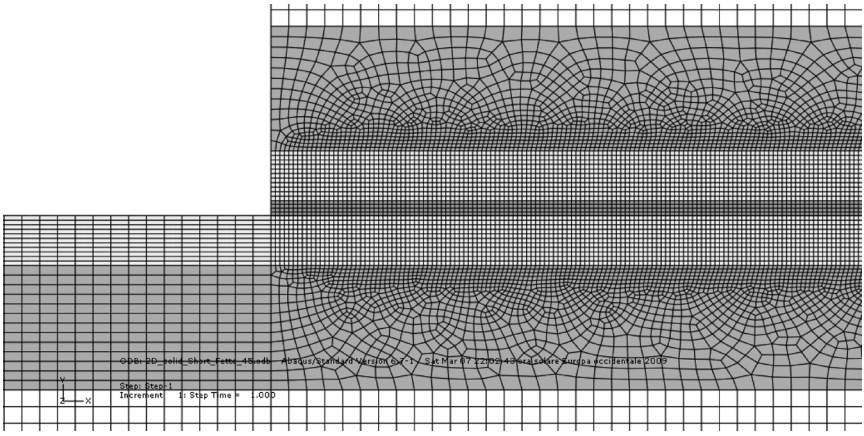

FIGURE 11 Detail of the 2-D solid mesh of a LS 25.4 joint.

constants reported in Section 2.2). A detail of the mesh used for the analysis is shown in Fig. 11. Linear static steps were conducted with constraints simulating the presence of the grips and using a reference point and a kinematic coupling to apply a concentrated load at one end of the specimen.

Stresses in the adhesive layer were evaluated in the mid plane, *i.e.*, 0.1 mm away from the stress singularity located at the corner between the adherend and the adhesive layer, at the location of the highly stressed node. In the case of SC 24.5 specimens, given the asymmetry of the stress distribution within the adhesive layer, the peak stress values were evaluated at the location of the most probable crack initiation site, which was observed on the right end of the overlap, *i.e.*, point B with reference to Fig. 1. Preliminary convergence analysis allowed the evaluation of the accuracy of the results provided by this analysis in the case of LS 25.4 and its sensitivity in the presence of the stress singularity. The four-element configuration provided an accuracy of 2% with respect to the reference stress evaluated by convergence analysis and this can be considered a good compromise between accuracy and calculation times.

Results of the FE analysis are reported in Table 4, in terms of peak elastic stress components acting at the most highly stressed node in the mid-plane of the adhesive layer for an applied load of 1 kN. Stress components reported in Table 4 are the shear stress acting tangentially to the mid-plane, the normal stress acting perpendicularly to the mid-plane, the Tresca equivalent stress, and the maximum principal stress. Fatigue tests results were then analyzed in terms of these

TABLE 4 Peak Stress Values Obtained with a 2-D Plane Strain Solid FE Model

Specimen type	Maximum shear stress	Maximum peel stress	Maximum Tresca	Maximum principal stress
LS 25.4	3.11 MPa/kN	5.86 MPa/kN	7.23 MPa/kN	7.10 MPa/kN
SC 25.4	2.20 MPa/kN	5.43 MPa/kN	6.14 MPa/kN	6.28 MPa/kN
LS 50.8	2.72 MPa/kN	5.27 MPa/kN	6.46 MPa/kN	5.68 MPa/kN
TC 110.8	2.19 MPa/kN	3.81 MPa/kN	4.97 MPa/kN	4.76 MPa/kN

local stress components by multiplying the maximum applied loads by the stress values reported in Table 4. The resulting peak stress values were normalized by dividing them by the fatigue strength of LS 25.4 joints at 100,000 cycles to failure in order to allow for direct comparison with the S-N curves reported in Fig. 3.

When the maximum shear stress is considered (Fig. 12), it appears that all experimental results collapse on a band of relatively low scatter with the exception of data points referring to SC 25.4 specimens. A similar behaviour is observed when the maximum normal stress (peel stress, Fig. 13) is taken as the reference stress. The larger deviation from a possible unique S-N curve in the case of both shear and peel stresses is mainly attributable to the SC 25.4 series. A possible explanation for this behaviour is the lower adhesion strength between adhesive and steel than between composite and adhesive, resulting

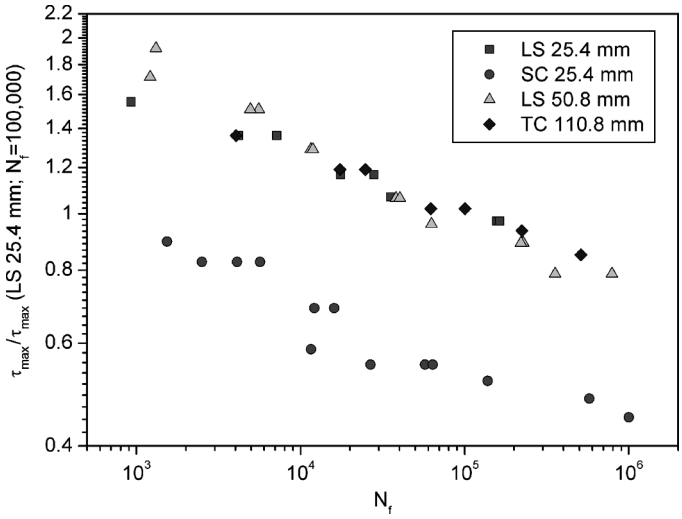

FIGURE 12 Fatigue test results in terms of maximum shear stress.

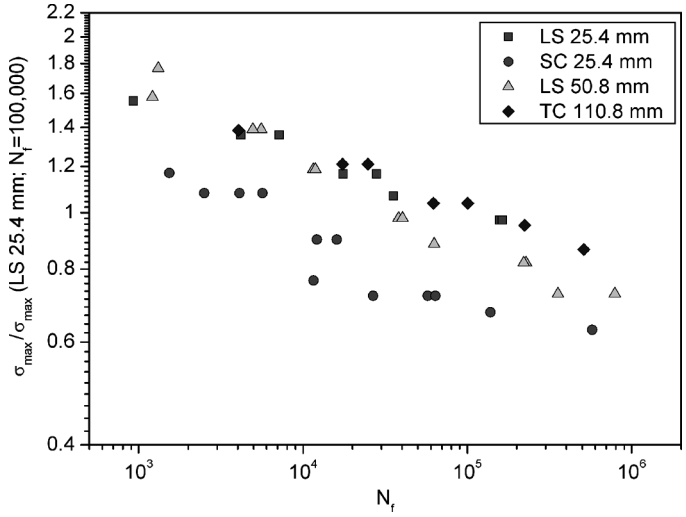

FIGURE 13 Fatigue test result in terms of maximum peel stress.

in early crack nucleation at the adhesive and steel interface, as shown in Fig. 6. A similar behaviour is observed when the S-N curve is expressed in terms of the Tresca equivalent stress (Fig. 14) and of the first principal stress (Fig. 15). The scatter of the Tresca and maximum principal values is similar to that of the maximum shear

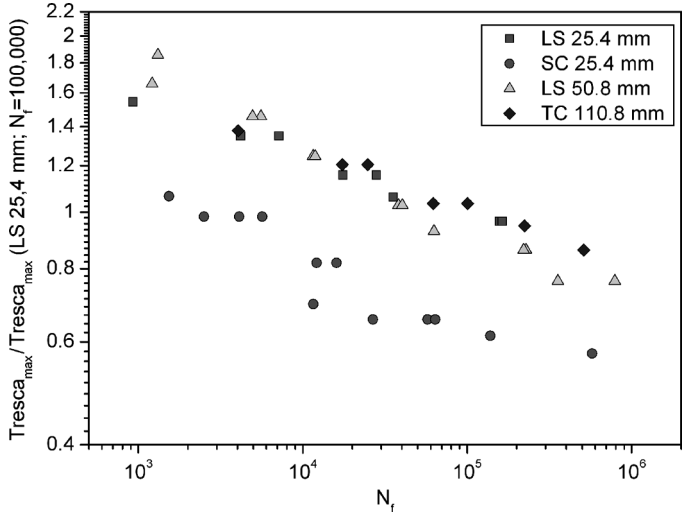

FIGURE 14 Fatigue test results in terms of Tresca stress.

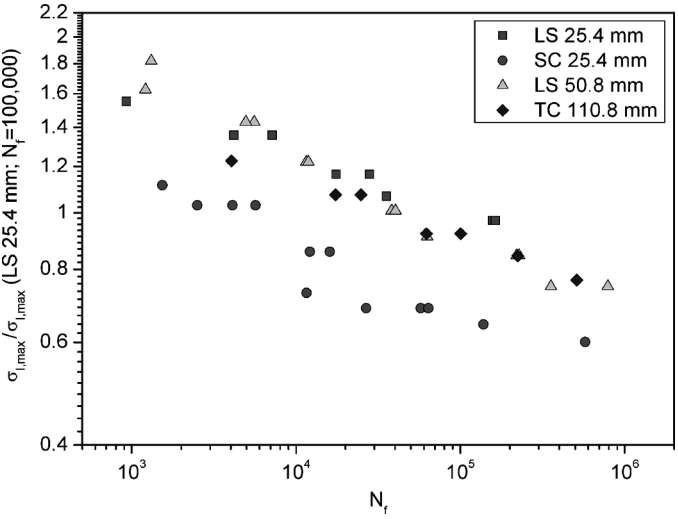

FIGURE 15 Fatigue test results in terms of the first principal stress.

and normal stresses: again, only the points referring to the results of the SC 25.4 series fall outside a relatively narrow band. Although the evaluation of the peak elastic stresses in the adhesive layer does not allow for taking into account the complex phenomena observed during the tests and the different fatigue crack propagation behaviour of joints of different shape, on the basis of these results it is then possible to propose as a criterion for the fatigue assessment of the all-composite joints, based on the peak values of the local stresses. With the specimen configurations we used, it is not possible to decide which stress component is most suitable for interpreting fatigue test results. The ratio between the peak values of the shear and the normal stresses (as well as between Tresca and maximum principal stresses) is very similar for all specimens, presumably because of the presence of an initial rise, irrespective of it height. Moreover, the use of adherends of different thicknesses, as in the case of SC 25.4 specimens, did not help to discriminate between the effect of normal and shear stresses, as it was supposed to thanks to the asymmetric stress distribution in the adhesive layer, presumably because of a lower interfacial strength of the adhesive-steel system.

At present, the validity of the proposed method is limited to the adhesive-substrate system used in the experiments (*e.g.*, the effect of the stacking sequence in the laminate still requires investigation) and the same mesh size is required for the evaluation of local stresses in the adhesive layer of the actual application and for the analysis of

test results. However, its simplicity makes it suitable for engineering applications. In this perspective, the use of 2-D solid elements for modelling the adhesive layer poses some limitations to the application to real parts, because of the large number of elements necessary for modelling the adhesive layer, even if sub-modelling techniques are employed. Therefore, a different approach based on the use of one single element in the thickness direction is also proposed in order to reduce the number of elements in the adhesive layer.

4.2. Use of One Single Element Along Thickness Directions

The adhesive layer was also modelled with only one element in the thickness direction (0.2 mm high) and mesh size of 0.05 mm along the glue line (equal to the 2-D solid mesh size), using both solid and cohesive 2-D elements. Details of the finite element mesh are shown in Fig. 16. A cohesive section with a continuum, linear elastic formulation was adopted when using cohesive elements. The use of this simplified constitutive model instead of a cohesive law is justified by the aim of replacing solid elements with cohesive ones and achieving computational efficiency in the perspective of analyzing larger, real parts. One quadratic, eight-node element was used in the case of solid elements. Stress

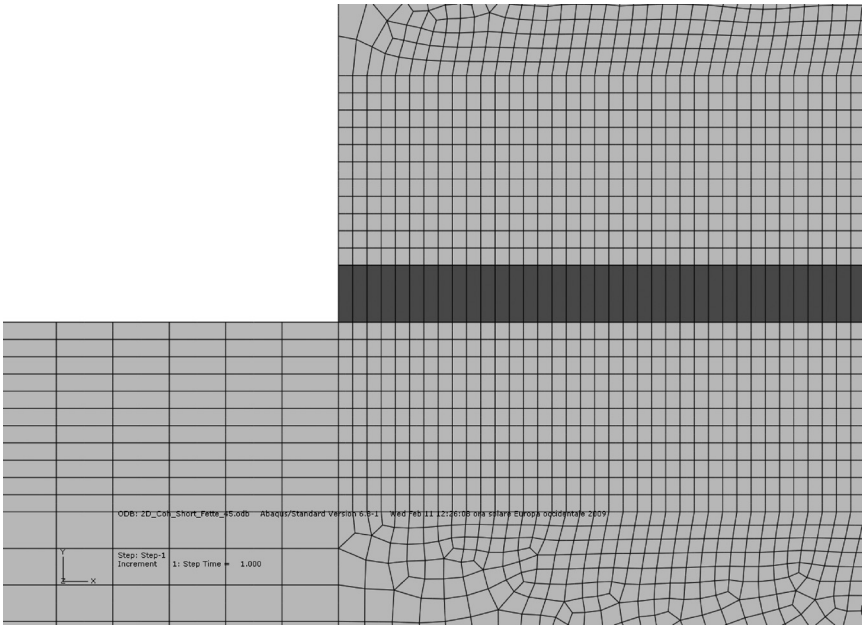

FIGURE 16 Detail of the adhesive layer modelled using cohesive elements.

TABLE 5 Comparison of Peak Stress Values Obtained with a 2-D Plane Strain Solid FE Models and 2-D Cohesive Elements (MPa/kN)

	2-D solid (four elements in thickness direction)				2-D cohesive (one element 0.05×0.2 mm)				2-D solid (one element 0.05×0.2 mm)			
Specimen type	τ_{max}	σ_{max}	Tresca_{max}	$\sigma_{I,max}$	τ_{max}	σ_{max}	Tresca_{max}	$\sigma_{I,max}$	τ_{max}	σ_{max}	Tresca_{max}	$\sigma_{I,max}$
LS 25.4	3.11	5.81	7.23	7.10	2.83	7.99	6.40	9.25	2.97	6.10	6.69	7.05
LS 50.8	2.72	5.27	6.46	5.68	2.47	7.24	5.63	8.27	2.59	5.55	6.00	6.26
TC 110.8	2.19	3.81	4.97	4.76	1.99	5.33	4.30	6.18	2.09	4.04	4.47	4.77

components were evaluated in the centroid of the highly stressed element and reported in Table 5, where results obtained with a finer mesh of four elements in the thickness direction are also reported in the first column as reference stresses for comparison (given the different behaviour of SC 25.4 specimens, they are not included in this analysis). Among all stress components, it appears that the values of the maximum shear stress are less sensitive to the mesh type and its size. Moreover, the values provided by cohesive elements are closer to the reference stresses than to those obtained using 2-D solid elements.

When used for plotting the graph of Fig. 17, although absolute values of the stress components are different from those obtained with structural elements, the maximum shear stress values display

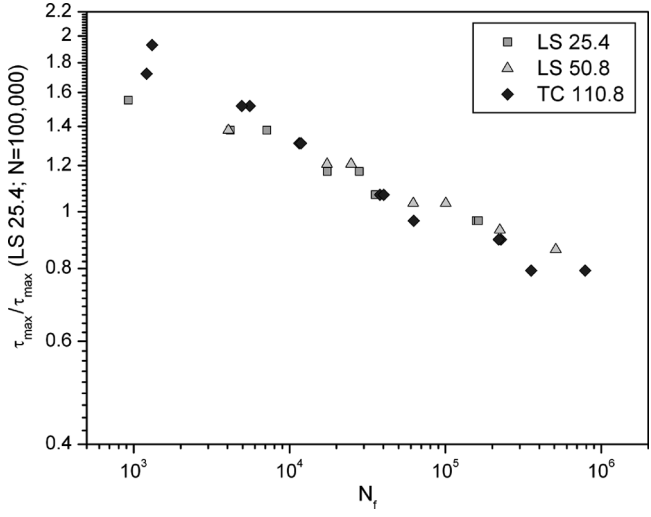

FIGURE 17 Fatigue test results in terms of Tresca stress evaluated using cohesive elements to model the adhesive layer.

the same correlation with the number of cycles to failure as in the case of models based on a finer mesh with four solid elements. Figure 17 refers to cohesive elements. Similar results can be obtained using a layer of one single linear 2-D solid element in the thickness

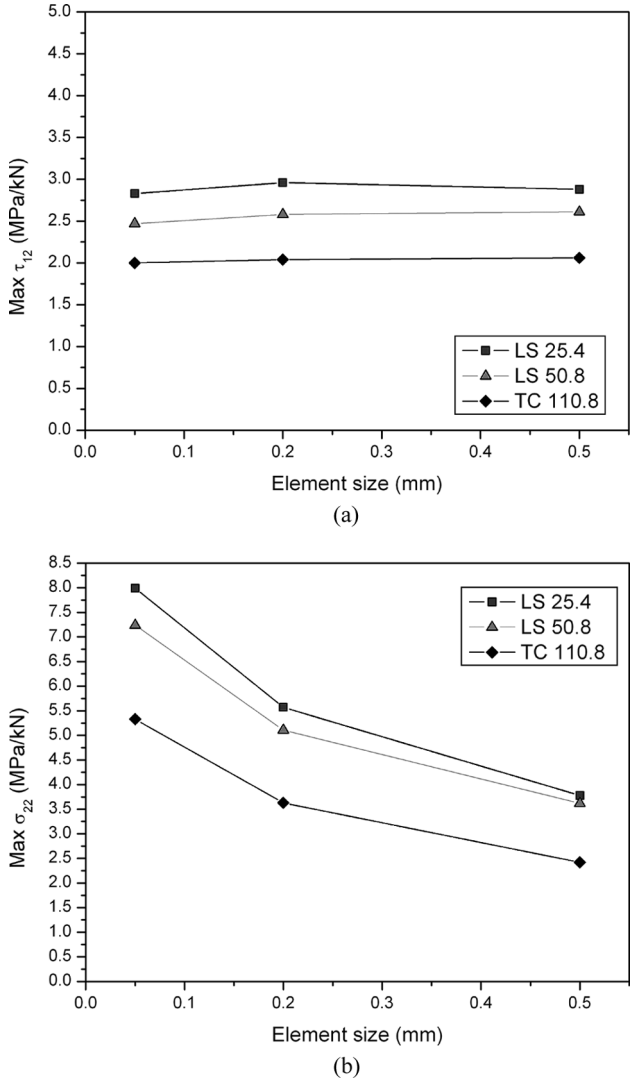

FIGURE 18 Sensitivity of the peak elastic stress values upon mesh size, using 2-D cohesive elements with a linear elastic constitutive model: (a) maximum shear stress, (b) maximum normal (peel) stress.

direction, as can be confirmed by comparing stress values reported in the second and third column, of Table 5. Moreover, the use of 2-D cohesive elements appears to be less prone to mesh size sensitivity. In fact, by increasing the dimension of the cohesive element from 0.05 to 0.5 mm, it appears that 2-D cohesive elements provide constant values of the maximum shear stress (Fig. 18a), whereas the peak peel stress is more affected by the mesh size (Fig. 18b). The use of cohesive elements, although in a simplified manner, *i.e.*, by adopting a linear elastic constitutive model, allows for defining a fatigue criterion based on the local maximum shear stress, which has low mesh sensitivity. By this method it is then possible to reduce the number of nodes in the adhesive layer and a possible method for simplifying the finite element mesh of adhesive layers in 3-D models is suggested.

5. CONCLUDING REMARKS

Fatigue tests were performed on thick composite adhesive lap joints having different shapes, different overlap lengths, and, in one case, with a steel adherend replacing one of the composite adherends. These configurations were designed in order to achieve different peak stress values in the adhesive layer. Fatigue tests provided four distinct S-N curves when expressed in terms of maximum applied forces. Local stresses were evaluated in the mid-surface of the adhesive layer by the finite element method, using 2-D structural elements, with linear elastic analyses. With the exception of the test series with specimens with dissimilar adherends, peak values of the shear and the normal (peel) stresses, as well as the Tresca equivalent stress and the maximum principal stress, displayed a close correlation with the number of cycles, irrespective of the type of joint. These results suggested that, although the crack propagation phase was the dominant mechanism, at least for total fatigue lives below 100,000 cycles, the peak elastic stresses could be adopted as an engineering tool for the fatigue assessment of joints in actual structures. In this perspective, preliminary investigations showed that it is possible to adopt a coarser mesh with one single element in the thickness direction, also using cohesive elements instead of solid elements, to model the adhesive layer and preserve the correlation between local stresses and number of cycles to failure. In this case, the peak shear stress proved to be less prone to mesh size sensitivity when evaluated with 2-D cohesive elements. The validity of the approach is at present limited to the laminate-adhesive system studied in this work and the suitability for different ply sequences needs further investigation.

REFERENCES

[1] de Goeij, W. C., van Tooren, M. J. L., and Beukers, A., *Materials and Design* **20**, 213–221 (1999).
[2] Ferreira, J. A. M., Reis, P. N., Costa, J. D. M., and Richardson, M. O. W., *Comp Sci Tech.* **62**, 1373–1379 (2002).
[3] Quaresimin, M. and Ricotta, M., *Comp Sci Tech.* **66**, 176–187 (2006).
[4] Crocombe, A. D. and Richardson, G., *Int. J. Adhesion and Adhesives* **19**, 19–27 (1999).
[5] Imanaka, M., Nakayama, H., Morikawa, K., and Nakamura, M., *Composite Structures* **31**, 235–241 (1995).
[6] Dessureault, M. and Spelt, J. K., *Int. J. Adhesion and Adhesives* **17**, 183–195 (1997).
[7] Hadavinia, H., Kinloch, A. J., Little, M. S. G., and Taylor, A. C., *Int. J. Adhesion and Adhesives* **23**, 449–461 (2003).
[8] Abdel Wahab, M. M., Ashcroft, I. A., Crocombe, A. D., and Smith, P. A., *Composites: Part A* **35**, 213–222 (2004).
[9] Quaresimin, M. and Ricotta, M., *Comp. Sci. Tech.* **66**, 647–656 (2006).
[10] Quaresimin, M. and Ricotta, M., *Int. J. Fatigue* **28**, 1166–1176 (2006).
[11] Abdel Wahab, M. M., Ashcroft, I. A., Crocombe, A. D., Hughes, D. J., and Shaw, S. J., *Composites: Part A* **32**, 59–69 (2001).
[12] Goglio, L., Rossetto, M., and Dragoni, E., *Int. J. Adhesion and Adhesives* **28**, 427–435 (2008).
[13] da Silva, L. F. M. and Adams, R. D., *Int. J. Adhesion and Adhesives* **27**, 227–235 (2007).